Acta Crystallographica Section B
Structural Science
ISSN 0108-7681

Structural investigation of the Na–Fe–Mo–O system

E. Muessig, K.G. Bramnik and H. Ehrenberg*

Darmstadt University of Technology, Institute for Materials Science, Petersenstrasse 23, D-64287 Darmstadt, Germany

Correspondence e-mail: ehrenberg@tu-darmstadt.de

Received 22 May 2003
Accepted 4 August 2003

Four new crystalline structures within the Na–Fe–Mo–O system are reported: sodium tetrairon pentamolydate (1), $NaFe_4(MoO_4)_5$, α-sodium diiron trimolybdate (2), α-$NaFe_2(MoO_4)_3$, β-sodium diiron trimolybdate (3), β-$NaFe_2(MoO_4)_3$, trisodium diiron trimolybdate (4), $Na_3Fe_2(MoO_4)_3$. All these structures belong to orthomolybdate class of compound and are described as networks of $[FeO_6]$ octahedra and $[MoO_4]$ tetrahedra. They are compared with each other and with other related structures.

1. Introduction

The following ternary compounds with different stoichiometric compositions have been reported for the Fe–Mo–O system and their phase relationships between 1173 and 1473 K have been discussed: $FeMoO_4$, Fe_2MoO_4, $Fe_2Mo_3O_8$ and $Fe_2Mo_3O_{12}$ (Koyama & Harada, 1994, and references therein). This ternary system offers a rich variety of possible compositions, structures and properties owing to the different formal oxidation states of Fe between +II and +III and of Mo between +IV and +VI.

Networks including $[FeO_6]$ octahedra, separated from each other by $[MoO_4]$ tetrahedra, are suitable model systems for magnetic interactions. Recently the correct ferrimagnetic structure of $Fe_2Mo_3O_{12}$ was predicted and experimentally verified, based on the assumption of increasing antiferromagnetic coupling strengths with increasing Fe—O—O and O—O—Fe angles along supersuperexchange paths (Ehrenberg *et al.*, 2003). An extension from qualitative to quantitative analyses of such coupling strengths could become feasible for a lower number of inequivalent exchange couplings by reducing the degree of links between $[FeO_6]$ octahedra because of separating alkaline ions in the structure. The 3*d* transition metal molybdates in general have been well known for their high activity and selectivity in some partial oxidation reactions since 1930 (Adkins & Peterson, 1931). For example, iron molybdates are used as heterogeneous catalysts in the oxidation of methanol to formaldehyde (Soares *et al.*, 2003, and references therein). Catalytic properties are very sensitive to structural details and the transition metal valences in the solid phase and, therefore, the insertion of alkaline metals into molybdates could be of interest for partial-oxidation catalysis. Furthermore, compounds with network structures built up from $[MoO_4]$ tetrahedra and $[FeO_6]$ octahedra are potential materials for the intercalation of alkaline metal ions because of possible changes in the formal oxidation states of Mo and Fe. Therefore, the consideration of quarternary compounds in alkaline 3*d*-transition-metal–molyb-

Table 1
Experimental details.

	(1)	(2)	(3)	(4)
Crystal data				
Chemical formula	$Fe_4Mo_5NaO_{20}$	$Fe_2Mo_3NaO_{12}$	$Fe_2Mo_3NaO_{12}$	$Fe_2Mo_3Na_3O_{12}$
M_r	1046.09	614.51	614.51	660.49
Cell setting, space group	Triclinic, $P\bar{1}$	Triclinic, $P\bar{1}$	Triclinic, $P\bar{1}$	Monoclininc, $C2/c$
a, b, c (Å)	6.9337 (3), 7.0196 (4), 17.8033 (8)	6.9253 (4), 6.9513 (4), 11.0600 (9)	6.8340 (10), 6.8930 (10), 11.667 (3)	12.646 (3), 13.685 (3), 7.206 (2)
α, β, γ (°)	87.468 (4), 87.615 (4), 79.090 (4)	80.205 (6), 83.679 (6), 80.818 (5)	76.23 (2), 75.78 (2), 87.76 (2)	90.00, 112.56 (3), 90.00
V (Å^3)	849.54 (7)	516.06 (6)	517.33 (17)	1151.6 (5)
Z	2	2	2	4
D_x (Mg m^{-3})	4.089	3.955	3.945	3.809
Radiation type	Mo $K\alpha$	Mo $K\alpha$	Mo $K\alpha$	Mo $K\alpha$
No. of reflections for cell parameters	10 278	3616	1012	507
θ range (°)	2.29–43.59	4.43–33.55	3.04–30.30	2.29–30.08
μ (mm^{-1})	7.00	6.39	6.37	5.81
Temperature (K)	293 (2)	293 (2)	293 (2)	293 (2)
Crystal form, colour	Prism, black	Prism, black	Prism, black	Prism, black
Crystal size (mm)	0.21 × 0.19 × 0.14	0.20 × 0.11 × 0.10	0.07 × 0.02 × 0.01	0.08 × 0.04 × 0.04
Data collection				
Diffractometer	Oxford Diffraction Xcalibur (TM) single-crystal X-ray diffractometer with sapphire CCD detector	Oxford Diffraction Xcalibur (TM) single-crystal X-ray diffractometer with sapphire CCD detector	Oxford Diffraction Xcalibur (TM) single-crystal X-ray diffractometer with sapphire CCD detector	Oxford Diffraction Xcalibur (TM) single-crystal X-ray diffractometer with sapphire CCD detector
Data collection method	Rotation method data acquisition using ω and φ scans(s)	Rotation method data acquisition using ω and φ scans(s)	Rotation method data acquisition using ω and φ scans(s)	Rotation method data acquisition using ω and φ scans(s)
Absorption correction	Numeric analytical	Numeric analytical	Numeric analytical	Numeric analytical
T_{min}	0.300	0.321	0.682	0.766
T_{max}	0.444	0.565	0.923	0.886
No. of measured, independent and observed reflections	37 235, 11 711, 9620	4259, 2705, 2454	4315, 2180, 1188	2221, 1055, 791
Criterion for observed reflections	$I > 2\sigma(I)$	$I > 2\sigma(I)$	$I > 2\sigma(I)$	$I > 2\sigma(I)$
R_{int}	0.035	0.027	0.061	0.043
θ_{max} (°)	43.6	33.5	30.3	26.4
Range of h, k, l	$-13 \Rightarrow h \Rightarrow 13$ $-13 \Rightarrow k \Rightarrow 13$ $-34 \Rightarrow l \Rightarrow 34$	$-10 \Rightarrow h \Rightarrow 9$ $-9 \Rightarrow k \Rightarrow 10$ $-14 \Rightarrow l \Rightarrow 14$	$-9 \Rightarrow h \Rightarrow 8$ $-9 \Rightarrow k \Rightarrow 9$ $-15 \Rightarrow l \Rightarrow 16$	$-13 \Rightarrow h \Rightarrow 13$ $-17 \Rightarrow k \Rightarrow 16$ $-8 \Rightarrow l \Rightarrow 8$
Refinement				
Refinement on	F^2	F^2	F^2	F^2
$R[F^2 > 2\sigma(F^2)]$, $wR(F^2)$, S	0.032, 0.078, 1.13	0.031, 0.081, 1.14	0.036, 0.129, 0.59	0.062, 0.196, 1.14
No. of relections	11 711 reflections	2705 reflections	2180 reflections	1055 reflections
No. of parameters	271	164	163	95
Weighting scheme	$w = 1/[\sigma^2(F_o^2) + (0.0311P)^2 + 1.1496P]$, where $P = (F_o^2 + 2F_c^2)/3$	$w = 1/[\sigma^2(F_o^2) + (0.0365P)^2 + 2.671P]$, where $P = (F_o^2 + 2F_c^2)/3$	$w = 1/[\sigma^2(F_o^2) + (0.1P)^2]$, where $P = (F_o^2 + 2F_c^2)/3$	$w = 1/[\sigma^2(F_o^2) + (0.1072P)^2 + 11.9291P]$, where $P = (F_o^2 + 2F_c^2)/3$
$(\Delta/\sigma)_{max}$	0.002	<0.0001	0.007	0.001
$\Delta\rho_{max}$, $\Delta\rho_{min}$ (e Å^{-3})	1.54, −2.29	0.98, −2.03	0.85, −0.90	1.34, −2.63
Extinction method	None	*SHELXL*	None	*SHELXL*
Extinction coefficient	–	0.0156 (8)	–	0.0003 (5)

Computer programs: *CrysAlis CCD* (Oxford Diffraction Limited, 2002*a*), *CrysAlis RED* (Oxford Diffraction, 2002*b*), *SHELXS* (Sheldrick, 1990), *SHELXL* (Sheldrick, 1997), *DIAMOND* (Brandenburg, 2001).

denum–oxide systems appears a necessary and promising approach to extend to investigations of the magnetic, catalytic, intercalation and ion-conducting properties of 3*d* transition metal molybdates. In this contribution we report on the crystalline structures in the Na–Fe–Mo–O system. Only three stoichiometric compositions have been previously mentioned in the literature: $NaFe(MoO_4)_2$ (Klevtsova, 1975), $Na_3Fe_2Mo_5O_{16}$ (Bramnik *et al.*, 2003) and $Na_2Fe_2(MoO_4)_3$ (Bruce & Miln, 1990). $NaFe(MoO_4)_2$ is built up from $[FeO_6]$ octahedra and $[MoO_4]$ tetrahedra in such a way that all the octahedra are linked to the tetrahedra by corner sharing and *vice versa* (Klevtsova, 1975). Layers of interconnected $[Mo_3O_{13}]$ clusters in $Na_3Fe_2Mo_5O_{16}$ are separated from each other by $[FeO_6]$ octahedra and $[MoO_4]$ tetrahedra (Bramnik *et al.*, 2003). $Na_2Fe_2(MoO_4)_3$ is described as a new phase, obtained by electrochemical sodium insertion into

$Fe_2(MoO_4)_3$ (Bruce & Miln, 1990). Only an expansion of the unit cell with respect to the $Fe_2(MoO_4)_3$ structure is reported, but no information about potential Na sites is provided.

Four additional crystalline phases in the Na–Fe–Mo–O system have recently been established by single-crystal X-ray analyses. Their structures are described and a scheme of Na–Fe orthomolybdate phases is proposed. The observed structure types are discussed in the light of the connectivities between octahedra and tetrahedra and compared with related structures.

2. Experimental

All samples have been obtained from the following reactants: Na_2MoO_4 (Aldrich, 98%), FeO (Aldrich, 99,9%), MoO_3 (Johnson Matthey, Grade A1), MoO_2 (Strem Chemicals, 99%) and Fe_2O_3 (Aldrich, 99.98%). Stoichiometric amounts of $NaFe_2(MoO_4)_3$ and $Na_4Fe(MoO_4)_3$, respectively, were mixed well in an agate mortar. The mixtures were then pressed into pellets and placed in alumina crucibles within evacuated (10^{-3} mbar) and sealed silica tubes. They were heated to 903 K and after 48 h slowly cooled down to room temperature. The reaction products appeared inhomogeneous under a light microscope and single crystals of different morphologies and colours have been isolated for single-crystal X-ray structure analyses. Diffraction data have been collected in ω- and φ-scans on the Xcalibur system from Oxford Diffraction, equipped with a CCD detector. An absorption correction was applied numerically, based on the shape of the crystals.

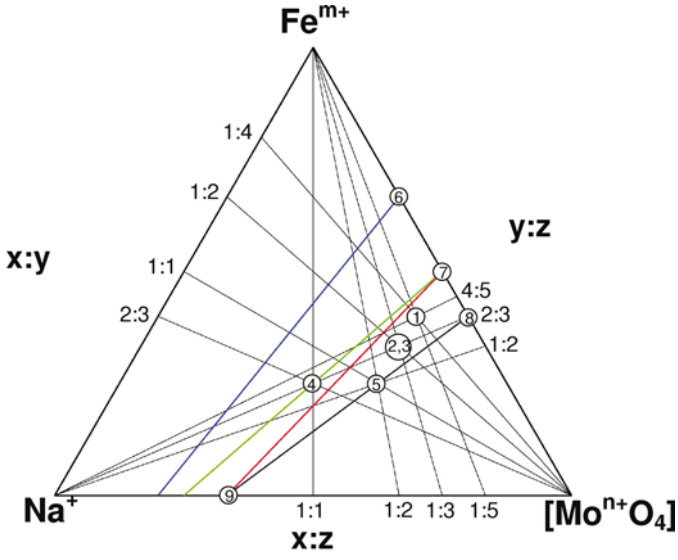

Figure 1
Scheme of crystalline phases $Na_xFe_y(MoO_4)_z$. The quarternary phases included are: (1) $NaFe_4(MoO_4)_5$, (2) α-$NaFe_2(MoO_4)_3$, (3) β-$NaFe_2(MoO_4)_3$, (4) $Na_3Fe_2(MoO4)_3$, (5) $NaFe(MoO_4)_2$, together with the ternary edge members (6) $Fe_2(MoO_4)$, (7) β-$Fe(MoO_4)$, (8) $Fe_2(MoO_4)_3$ and (9) $Na_2(MoO_4)$. The coloured lines mark the ranges of composition with the same formal oxidation state m+ of Fe and n+ of Mo (blue: $m = 2, n = 4$; green: $m = 3, n = 5$; red: $m = 2, n = 6$; black: $m = 3, n = 6$). Only the region between the blue and black lines is of relevance for the orthomolybdate structures.

Structure solutions and refinements were performed using *SHELXS* (Sheldrick, 1986) and *SHELXL* (Sheldrick, 1993), respectively.

3. Results

Four new phases could be established by single-crystal X-ray structure determination: (1) $NaFe_4(MoO_4)_5$, (2) α-$NaFe_2(MoO_4)_3$, (3) another polymorph with the same composition, β-$NaFe_2(MoO_4)_3$, and (4) $Na_3Fe_2(MoO_4)_3$. Experimental details are given in Table 1 and the atomic parameters have been deposited.[1]

4. Discussion

All four structures are composed of networks of $[FeO_6]$ octahedra and $[MoO_4]$ tetrahedra. The oxygen ions belong to exactly one $[MoO_4]$ tetrahedron, so that the general sum formula is $Na_xFe_y(MoO_4)_z$.

Accordingly, all four newly established structures include isolated $[MoO_4]$ tetrahedra only and, therefore, fit into the proposed scheme of orthomolybdates in Fig. 1. Black lines mark the constant ratios x:y, y:z and z:x, respectively, while the coloured lines refer to the specific formal oxidation states of Fe and Mo. The known phase $NaFe(MoO_4)_2$ also fits into this scheme as well as the ternary edge members Na_2MoO_4 (Lindqvist, 1950), β-$FeMoO_4$ (Sleight *et al.*, 1968), Fe_2MoO_4 (Abe *et al.*, 1972) and $Fe_2(MoO_4)_3$ (Chen, 1979). The only quarternary phase in the Na–Fe–Mo–O system which does not belong to the class of orthomolybdates and, therefore, not to the scheme of Fig. 1, is $Na_3Fe_2Mo_5O_{16}$, in which three $[MoO_6]$ octahedra are connected by edge-sharing to $[Mo_3O_{13}]$ clusters as in $Fe_2Mo_3O_8$. In α-$FeMoO_4$ and $FeMoO_4$-II the molybdenum ions are coordinated octahedrally.

In contrast to $[MoO_4]$ tetrahedra, which are in the orthomolybdates never linked to each other by common O atoms, the $[FeO_6]$ octahedra in the $Na_xFe_y(MoO_4)_z$ phases often form dimers by edge-sharing. The different structure types have several motifs in common, especially the characteristic layers which are formed. The first structure described in detail is one of the two $NaFe_2(MoO_4)_3$ polymorphs (α-), see Fig. 2. Two types of layers, (*A*) and (*B*), parallel to the *ab* plane are formed, see Figs. 3 and 4, and the structure is completed by inversion symmetry. The sequence of constituting layers is *A*–*B*–*B*′–*A*–*B*–*B*′–*A* along the *c* axis, with *B*′ obtained from *B* by inversion symmetry. The centrosymmetric layers $A' = A$ are built up from edge-sharing $[FeO_6]$ octahedra dimers, connected to each other by corner-sharing with $[MoO_4]$ tetrahedra, see Fig. 3. All Fe–Fe vectors in the dimers are parallel to each other and to one face of the linking $[MoO_4]$ tetrahedra. Every fourth O atom of the $[MoO_4]$ tetrahedra points upwards and then downwards, alternating along $[1\bar{1}0]$. The other type of constituting layer, *B*, includes eight-

[1] Supplementary data for this paper are available from the IUCr electronic archives (Reference: OS5002). Services for accessing these data are described at the back of the journal.

membered rings of alternating corner-sharing [MoO_4] tetrahedra and [FeO_6] octahedra, see Fig. 4. The Na ions are situated in the centres of these rings.

The crystal structure of $NaFe_4(MoO_4)_5$ is very similar, see Fig. 5, but with one more constituting layer type. The main difference between layer types *C* and *A* is the lack of inversion symmetry, reflected in the orientations of the [MoO_4] tetrahedra: in the centrosymmetric layer *A*, half of the tetrahedra points upwards and downwards along the *c* axis in an alternating manner, while all the [MoO_4] tetrahedra point downwards in layers *C* and upwards in layers *C*′. Note that the origin in $NaFe_4(MoO_4)_5$ is shifted by ($\frac{1}{2}$,0,0) compared with the corresponding layers in Figs. 3 and 4 of α-$NaFe_2(MoO_4)_3$.

The other polymorph of $NaFe_2(MoO_4)_3$ (β-) is also built up from the layer type *B* and another type *D*, see Fig. 6. This new layer type *D* parallel to the *ab* plane is formed again by eight-membered rings of alternating [MoO_4] tetrahedra and [FeO_6] octahedra, as in Fig. 4, but without the Na ions in the centre of its rings. An alternative description of this structure is based on only one layer type *E* which is parallel to the *bc* plane, see Figs. 6 and 7. Again, edge-sharing [FeO_6] octahedra dimers are

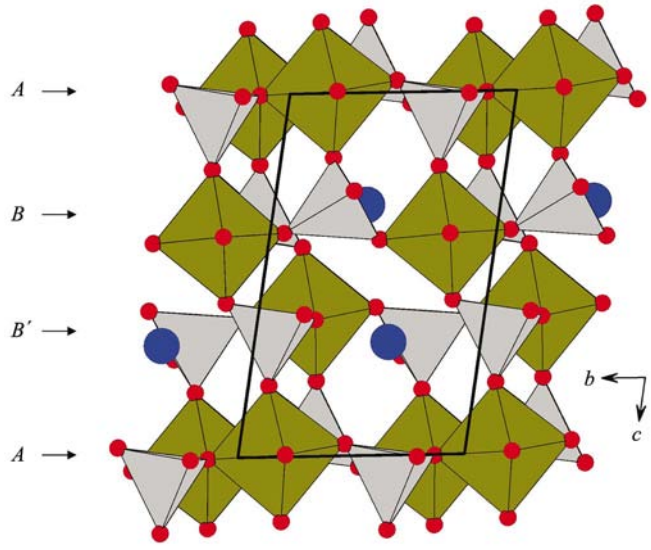

Figure 2
Crystal structure of α-$NaFe_2(MoO_4)_3$.

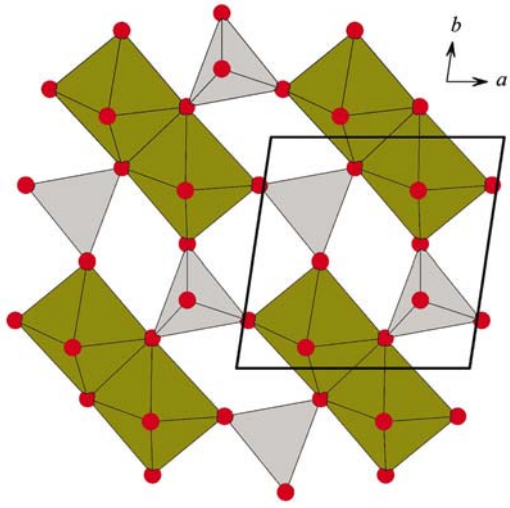

Figure 3
Constituting layer type *A*.

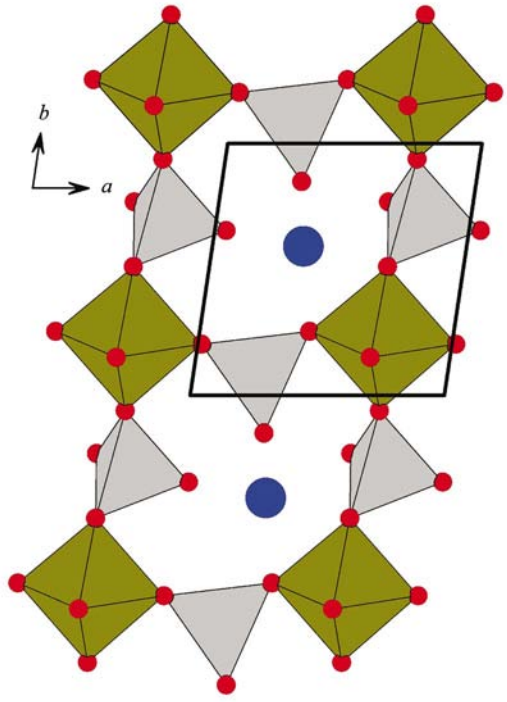

Figure 4
Layer type *B*.

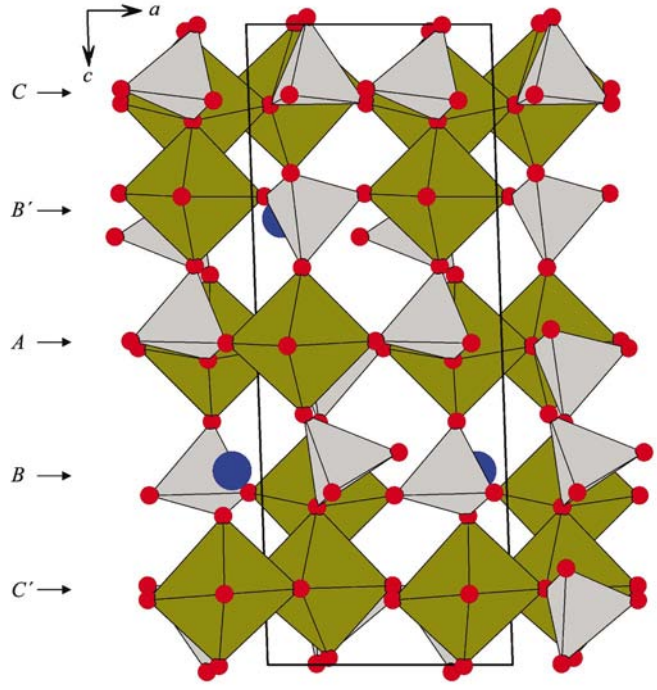

Figure 5
Crystal structure of $NaFe_4(MoO_4)_5$.

linked by [MoO_4] tetrahedra and all Fe–Fe vectors in the dimers are parallel to each other. However, chains of dimers along the *b* axis are separated from each other along the *c* axis by Na ions. The crystal structure results from successive layers *E* and its inverse *E*′ along the *a* axis. The crystal structure of $Na_3Fe_2(MoO_4)_3$ includes layers of edge-sharing [FeO_6] octahedral dimers again linked by [MoO_4] tetrahedra, but the Fe–Fe vectors of the dimers are only parallel to each other along the *c* axis while running in a zigzag manner along the *b* axis, see Fig. 8. These layers of type *F* are separated from each other by a layer type *G*, which includes only Na ions and [MoO_4] tetrahedra. The sequence *G*–*F*–*G*–*F*′–*G*–*F*–*G*–*F*′–*G* along the *a* axis results in the layered structure of $Na_3Fe_2(MoO_4)_3$, see Fig. 9, with a two-dimensional network of octahedral dimers, separated by Na ions, situated in channels along [001], [01$\bar{1}$] and [011], respectively.

The $Na_3Fe_2(MoO_4)_3$ structure is related to the alluaudite-type structure (Moore, 1971) which also contains the layer type *F* and Na ions situated in channels. Furthermore, the $Na_3Fe_2(MoO_4)_3$ structure is isotypic with $Na_3In_2(AsO_4)_3$ (Lii & Ye, 1997; Khorari *et al.*, 1997). A similar zigzag arrangement of the dimers is also known for $Na_4Cu(MoO_4)_3$ with severely Jahn-Teller distorted [CuO_6] octahedra (Klevtsova *et al.*, 1991). The much lower three-dimensional transition-metal-to-alkaline ratio, however, results in a one-dimensional chain only. A similar chain is found in $K_4Mn(MoO_4)_3$ (Solodovnikov *et al.*, 1998), but with a parallel arrangement of the dimers, as in the above-described layer *E* in β-$NaFe_2(MoO_4)_3$, only with more potassium sites between the chains instead of sodium. In the Na–Fe–Mo–O system, different degrees of connectivity are realised: [FeO_6] octahedra are linked by corner-sharing with [MoO_4] tetrahedra to a two-dimensional network of monomers, separated by Na ions, in $NaFe(MoO_4)_2$ (Klevtsova, 1975). A one-dimensional chain of dimers is observed in β-$NaFe_2(MoO_4)_3$, and two-dimensional dimer networks are observed in α-$NaFe_2(MoO_4)_3$ and $Na_3Fe_2(MoO_4)_3$. In $NaFe_4(MoO_4)_5$ even trimers of edge-sharing [FeO_6] octahedra exist. These connectivity schemes are of relevance for the magnetic interactions in these systems: edge-sharing octa-

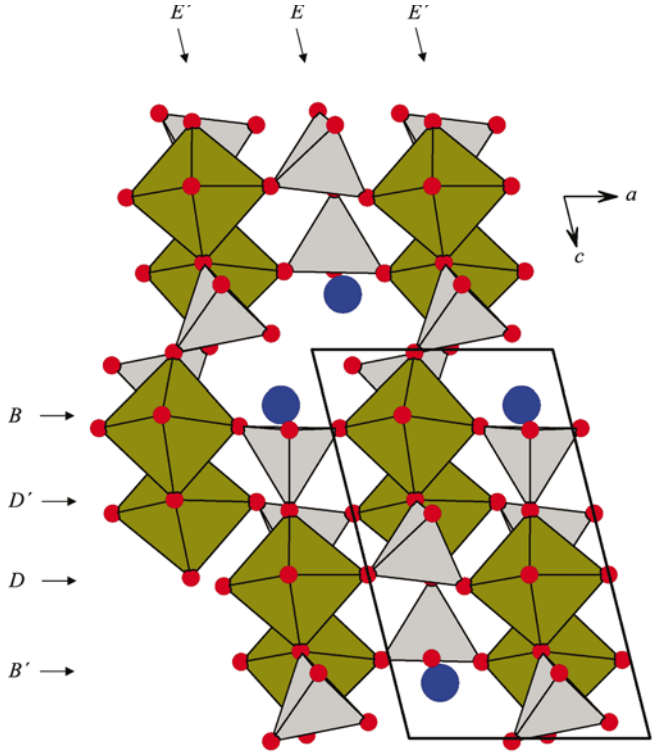

Figure 6
Crystal structure of β-$NaFe_2(MoO_4)_3$.

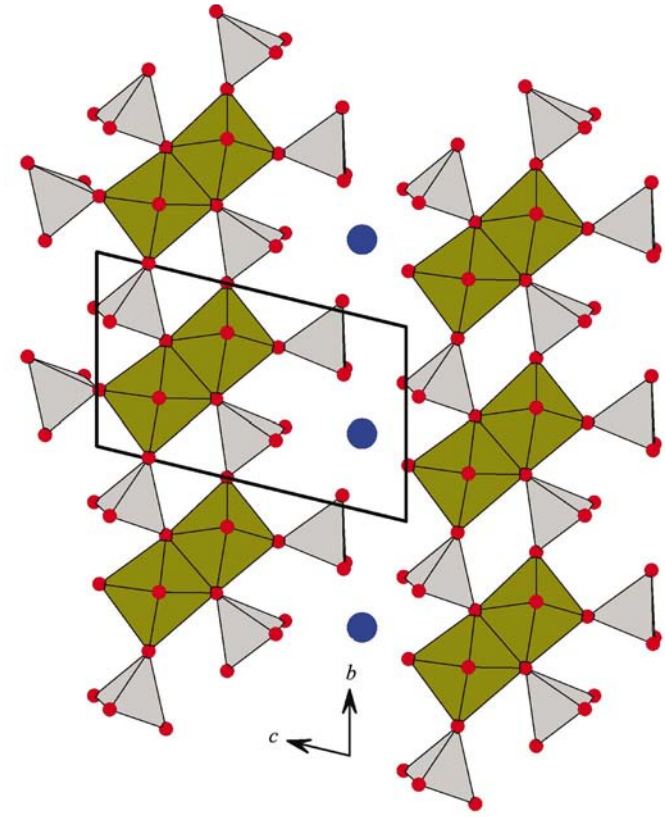

Figure 7
Layer type *E*.

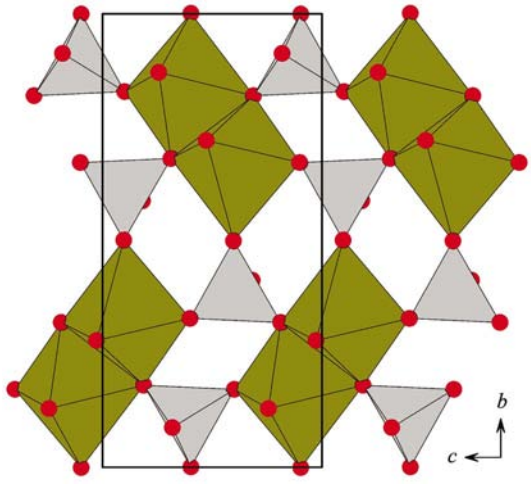

Figure 8
Layer type *F*.

Table 2
Structural characteristics of alkaline 3*d* transition-metal orthomolybdates.

Compound	Connectivity of [FeO_6] octahedra and [MoO_4] tetrahedra	Arrangements of [FeO_6] octahedra	Reference
$Na_3Fe_2(MoO_4)_3$	Three-dimensional network	Dimers, canted	This work
α-$NaFe_2(MoO_4)_3$	Three-dimensional network	Dimers, parallel	This work
β-$NaFe_2(MoO_4)_3$	Three-dimensional network	Dimers, parallel	This work
$NaFe_4(MoO_4)_5$	Three-dimensional network	Dimers, parallel	This work
$Fe_2(MoO_4)_3$	Three-dimensional network	Monomers	Chen (1979)
$NaFe(MoO_4)_2$	Layers	Monomers	Klevtsova (1975)
$Na_4Cu(MoO_4)_3$	Infinite ribbons	Dimers, canted	Klevtsova *et al.* (1991)
$K_4Mn(MoO_4)_3$	Infinite ribbons	Dimers, parallel	Solodovnikov *et al.* (1998)

hedra allow for superexchange interactions, but additional supersuperexchange couplings according to Fe–O–O–Fe paths along the bridging [MoO_4] tetrahedra have also to be considered.

$NaFe_4(MoO_4)_5$ is isotypic to $NaMg_3In(MoO_4)_5$ (Klevtsova *et al.*, 1993). In the latter compound a random distribution of Mg and In on one site in the ratio 3:1 is reported. This supports a formal oxidation state of +6 for Mo in $NaFe_4(MoO_4)_5$ and an average of 2.25 for Fe. The Fe—O and Mo—O bond lengths in all the structures under consideration are very similar and do not allow the assignment of a formal oxidation state based on valence-bond sums or any conclusions about the high- or low-spin states of the Fe ions.

The Na coordinations of the compounds are derived with respect to the Na—O distances and the resulting geometry of the polyhedra. In contrast to iron and molybdenum, a rich variety of Na coordination polyhedra is observed: for α-$NaFe_2(Mo_4)_3$ a fivefold coordination is found and for the other polymorph, β-$NaFe_2(MoO_4)_3$, an eightfold coordination close to a double-capped trigonal prism is found. $Na_3Fe_2(MoO_4)_3$ has three different Na sites, with two [NaO_6] polyhedra forming distorted octahedra and one Na site which is square-planar. For $NaFe_4(MoO_4)_5$ a fivefold Na—O coordination is observed.

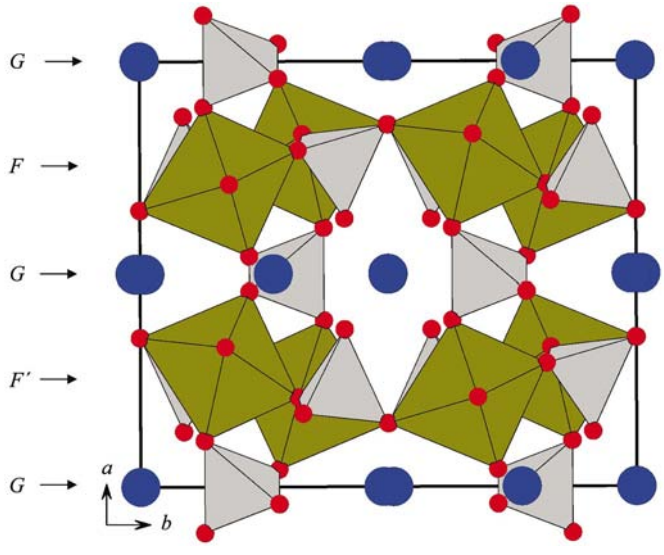

Figure 9
Crystal structure of $Na_3Fe_2(MoO_4)_3$.

Based on the very different environments, the Na ions can be considered as just being spacers between connected [FeO_6] octahedra and [MoO_4] tetrahedra, so that different connectivity schemes result, see Table 2. Accordingly, all four newly established structures represent three-dimensional networks of octahedra and tetrahedra as in $Fe_2(MoO_4)_3$. In contrast, layers of octahedra and tetrahedra are separated by Na ions in $NaFe(MoO_4)_2$. The higher alkaline content in $Na_4Cu(MoO_4)_3$ and $K_4Mn(MoO_4)_3$ results in ribbons of octahedra and tetrahedra. A similar structure is also expected in the Na–Fe–Mo–O system and, therefore, further studies are needed to complete the scheme of the orthomolybdates and to determine the magnetic, catalytic and ion conducting properties of the phases involved.

The authors thank Professor Dr H. Fuess for valuable discussions and the *Fonds der Chemischen Industrie* for financial support.

References

Abe, M., Kawachi, M. & Nomura, S. (1972). *J. Phys. Soc. Jpn*, **33**, 1296–1302.
Adkins, H. & Peterson, W. R. (1931). *J. Am. Chem. Soc.* **5**, 1512–1520.
Bramnik, K. G., Muessig, E. & Ehrenberg, H. (2003). *J. Solid State Chem.* In the press.
Brandenburg, K. (2001). *DIAMOND*. Version 2.1e. Crystal Impact GbR, Bonn, Germany.
Bruce, P. G. & Miln, G. (1990). *J. Solid State Chem.* **89**, 162–166.
Chen, H. Y. (1979). *Mater. Res. Bull.* **14**, 1583–1590.
Ehrenberg, H., Bramnik, K. G., Muessig, E., Buhrmester, T., Weitzel, H. & Ritter, C. (2003). *J. Magn. Magn. Mater.* **261**, 353–359.
Khorari, S., Rulmont, A. & Tarte P. (1997). *J. Solid State Chem.* **134**, 31–37.
Klevtsova, R. F. (1975). *Dokl. Akad. Nauk SSSR*, **221**, 1322–1325.
Klevtsova, R. F., Borisov, S. V., Bliznyuk, N. A., Glinskaya, L. A. & Klevtsov, P. V. (1991). *J. Struct. Chem.* **32**, 885–893.
Klevtsova, R. F., Vasiliev, A. D., Kozhevnikova, N. M., Glinskaya, L. A., Kruglik, A. I. & Kotova, I. Y. (1993). *J. Struct. Chem.* **34**, 784–788.
Koyama, K. & Harada, T. (1994). *J. Jpn Inst. Metals*, **58**, 1401–1407.
Lii, K.-H. & Ye, J. (1997). *J. Solid State Chem.* **131**, 131–137.
Lindqvist, I. (1950). *Acta Chem. Scand.* **4**, 1066–1074.
Moore, P. B. (1971). *Am. Mineral.* **56**, 1955–1975.
Oxford Diffraction (2002*a*). *CrysAlis CCD*. Version 1.170.14. Oxford Diffraction, Oxford, UK.
Oxford Diffraction (2002*b*). *CrysAlis RED*. Version 1.170.14. Oxford Diffraction, Oxford, UK.
Sheldrick, G. M. (1986). *SHELX*86. University of Göttingen, Germany.
Sheldrick, G. M. (1993). *SHELX*93. University of Göttingen, Germany.
Sleight, A. W., Chamberland, B. L. & Weiher J. F. (1968). *Inorg. Chem.* **7**, 1093–1098.
Soares, A. P. V., Portela, M. F., Kiennemann, A. & Hilaire, L. (2003). *Chem. Eng. Sci.* **58**, 1315–1322.
Solodovnikov, S. F., Klevtsov, P. V., Solodovnikova, Z. A., Glinskaya, L. A. & Klevtsova, R. F. (1998). *J. Struct. Chem.* **39**, 230–237.